Composite Structures 124 (2015) 29–34

Contents lists available at ScienceDirect

Composite Structures

journal homepage: www.elsevier.com/locate/compstruct

Optimization of transparent laminates for specific energy dissipation under low velocity impact using genetic algorithm

G.O. Antoine, R.C. Batra *

Department of Biomedical Engineering and Mechanics, M/C 0219, Virginia Polytechnic Institute and State University, Blacksburg, VA 24061, USA

ARTICLE INFO

Article history:
Available online 6 January 2015

Keywords:
Low-velocity impact
Genetic algorithm
Optimal design
Energy dissipation

ABSTRACT

We employ a genetic algorithm to maximize the energy dissipated per unit areal density in laminates composed of layers of poly-methyl-metha-acrylate (PMMA), adhesive and polycarbonate (PC) impacted at low velocity by a rigid hemi-spherical nosed cylinder. Sources of energy dissipation considered are plastic deformations of the PC and the PMMA, cracking of the PMMA, viscous deformations of the adhesive, and the energy used to deform failed elements that are deleted from the analysis domain. Some of the challenging issues are appropriate constitutive relations for the three materials, failure criteria, and numerical techniques to accurately analyze finite deformations of different constituents. We model the PC and the PMMA as thermo-elasto-visco-plastic materials with constitutive relations proposed by Mulliken and Boyce and modified by Varghese and Batra, the adhesive as a visco-elastic material, and use the commercial finite element software LS-DYNA in which these material models have been implemented as user defined subroutines. This software is coupled with a genetic algorithm to optimize the layup of the PC, the PMMA and the adhesive layers of the same thickness under the constraints that the top and the bottom layers are not adhesive, the PC and the PMMA layers must have an adhesive layer between them, and the total number of layers is fixed.

1. Introduction

Optimizing the impact performance of laminated structures can save mass and hence cost. Furthermore, using a computational algorithm to optimize the design can minimize the number of prototypes to be built and tested. Florence [1] gave an analytical expression for estimating the ballistic limit of a two-component ceramic-faced armor as a function of the impactor mass and radius, and of the ply thicknesses, mass densities, failure strains and the ultimate tensile strength of the armor materials. Ben-Dor et al. [2] modified the expression by scaling the predicted ballistic limit with a parameter that is determined from the available experimental data and formulated a condition of optimality for the armor design for constant areal density but the thicknesses of the two plates as variables. Ben-Dor et al. [3] used the modified expression to optimally design armor, provided closed-form simple solutions to the optimization problem and showed that the range of possible designs giving almost identical ballistic performance is broad. Hetherington [4] used Florence's [1] expression to optimally design a ceramic/aluminum armor by keeping the areal density constant and analytically finding the range of thickness ratios for the highest ballistic limit of the armor. Hetherington found that the impact performance is better when the ceramic tile is thicker than the backing plate, and verified the optimal design through physical tests.

Here we use a genetic algorithm (GA) to maximize the energy dissipated during the low-velocity impact (below the perforation limit) of a clamped rectangular laminate of a given areal density. The laminate is composed of different layers of poly-methyl-metha-acrylate (PMMA), adhesive and polycarbonate (PC). Since the mass density of the three materials is nearly the same, the design variables are the arrangement of layers under the constraint that the adhesive layer cannot be one of the major surfaces and the PMMA and the PC layers must have an adhesive layer between them. The problem has been simplified by assuming that each layer is of the same thickness, and the adjacent layers are perfectly bonded to each other. Thus only the arrangement (or the layup) of layers is to be determined. This optimization problem is similar to that of a fiber-reinforced laminate with the fiber orientation angle in each layer as the design variable; e.g. see Batra and Jin [5]. Qian and Batra [6], Goupee and Vel [7] and Batra [8] studied the spatial variation of elastic moduli to optimize either the fundamental frequency or the stress distribution in a structure. The optimization problem of minimizing a laminate weight while fulfilling

* Corresponding author. Tel.: +1 540 231 6051; fax: +1 540 231 4574.
E-mail addresses: antoineg@vt.edu (G.O. Antoine), rbatra@vt.edu (R.C. Batra).

http://dx.doi.org/10.1016/j.compstruct.2014.12.066
0263-8223/

requirements of the strength, fundamental frequency, buckling load and/or strain limit have been studied, amongst others, by Nagendra et al. [9,10], Gantovnik et al. [11], Nagendra et al. [12], Kogiso et al. [13], Gantovnik et al. [14], and Malott et al. [15]. Another class of problems is to maximize a structural property, typically the buckling load, while keeping the number of plies or the weight constant; e.g. see Soremekun et al. [16].

Punch et al. [17] and Punch et al. [18] used a GA to optimally design a laminated beam for the maximum energy absorption when a point load is suddenly applied at the center of the top surface. Poirier et al. [19] used the GA to analyze a multi-objective problem for a laser welded steel beam.

The major contribution of the present work is in applying the GA technique to a transient coupled thermo-elasto-visco-plastic problem involving finite deformations, material failure, cracking and significant plastic deformations.

2. Problem definition and method

2.1. Initial-boundary-value problem

A schematic sketch of the impact problem studied is depicted in Fig. 1. A $L_1 \times L_2$ rectangular clamped laminated plate made of n layers of thickness h_1 through h_n and total thickness $h = \Sigma h_i$ is impacted at normal incidence by a hemispherical nosed rigid impactor of mass m moving at velocity v_0. The layers are made of PMMA, PC, DFA4700 or IM800A. The PMMA and the PC are glassy transparent polymers, while the DFA4700 and the IM800A are transparent viscous adhesives. The thermo-elasto-visco-plastic material model developed by Mulliken and Boyce [20] and modified by Varghese and Batra [21] is used for the PMMA and the PC. The DFA4700 and the IM800A are modeled as nearly incompressible viscous rubbery materials with the elastic response represented by the Ogden energy potential and the viscoelastic response by a hereditary type integral e.g., see [30]. Effects of both geometric and material nonlinearities are considered. The different layers are assumed to be perfectly bonded and the continuity of displacements and surface tractions is imposed between adjacent layers. Thus successive layers made of the same material are equivalent to one thick layer. The mass densities of the PMMA, the PC, the DFA4700 and the IM800A are taken to equal 1.2, 1.2, 1.1 and 1.04 g/cm^3. The constitutive relations and values of material parameters for these materials are given in [20–22]. Similarly, partial differential equations governing deformations of the system, and the initial and the boundary conditions are summarized in [22]. In the present work we take $L_1 = L_2 = 120$ mm, $h = 4.0$ mm, $n = 12$ and h_1 through $h_n = 0.33$ mm. The spherical rigid impactor of radius $R = 5$ mm and mass $m = 35$ g impacts the plate center at $v_0 = 20$ m/s.

2.2. Optimization problem

Our goal is to find the material of the 12 layers that will maximize the energy dissipated during the impact. Whereas one usually considers the constraint of constant areal density (e.g., see [2–4]), here the layers are assumed to have fixed thickness. Since mass densities of the materials vary between 1.04 and 1.20 g/cm^3, variations in the areal density among the layers are small. We impose the constraint that layers 1 and 12 are made of either PMMA or PC and that the PMMA and the PC layers within the laminated plate cannot have common interfaces but must be bonded with an adhesive layer.

We assign each material an integer between 1 and 4 as listed in Table 1 and denote the energy dissipation by the function f. Thus f is a function of x_1 through x_{12}, where the x_i is the material of the ith layer, and the optimization problem is:

$$\text{maximize} \quad f(x_1, x_2, \ldots, x_{12}) \tag{1a}$$
$$\text{subject to} \quad x_1 = 1 \quad \text{or} \quad x_1 = 4 \tag{1b}$$
$$x_{12} = 1 \quad \text{or} \quad x_{12} = 4 \tag{1c}$$
$$|x_{i+1} - x_i| \le 2 \quad \text{for } 1 \le i \le 11 \tag{1d}$$

With constraints defined by Eq. (1b)–(1d) there is a total of 885,922 admissible designs. The computational cost of evaluating the fitness of each design is unrealistically high which motivates the use of an optimization algorithm to explore the design space.

2.3. Genetic algorithm

The optimization problem described by Eq. (1a)–(1d) is solved by using a GA. A GA is a direct search method that uses ideas based on natural selection to explore the search space for finding a global optimum. Population initialization, parent selection, crossover, mutation and selection of the fittest are common elements in most GAs, e.g. see [16] and [23]. A GA generally involves the following steps: (i) generate an initial population of individuals, (ii) develop a scheme to select members for mating in the existing population with preference given to the fittest individuals (individuals with the highest objective function value), (iii) create children through mating, and (iv) replace the existing population. We follow guidelines presented in Refs. [16,23] for selecting individuals for mating, generating children, and enforcing the constraints. A random number generator is used to simulate approximate uniform distribution where evolution is directed by random numbers. The function of the GA is schematically depicted in Fig. 2.

2.3.1. Selection strategy for new parents

In a typical GA after a new population is formed the previous population is killed and is replaced by the new one. However, there is no guarantee that an individual in the new generation has higher fitness than that of the best individual in the previous one. In other

Table 1
Coding of the materials.

Material	PMMA	DFA4700	IM800A	PC
Code (value of the variable x_i)	1	2	3	4

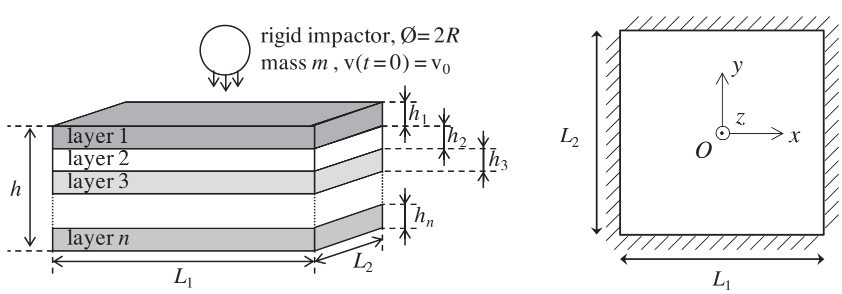

Fig. 1. Sketch of the impact problem studied.

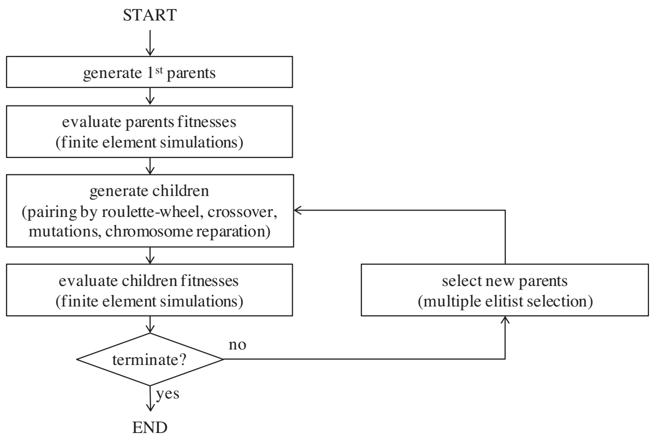

Fig. 2. Schematic representation of the genetic algorithm.

words, there is no guarantee that the new generation is an improvement over the previous one in terms of fitness. Elitist selection strategies remedy this problem by keeping information about the best individual(s) from the previous generation and preserving the largest value of the objective function. In the present work we rely on two multiple elitist selection strategies, ME_1 and ME_2, introduced by Soremekun et al. [16]. These strategies and their comparison to the simple elitist selection strategy are briefly described below for the sake of completeness.

After children are created from the parent population as described in the next section their fitnesses are evaluated. In a typical GA they become the new parent population and the process is repeated. The elitist selection strategy modifies this simple strategy in replacing the child with the lowest fitness by the best parent which is thus carried over to the next generation. All children (except the weakest one) and the best parent become the new parents from which the new children are born. Thus information about the best individual is preserved and the algorithm is prevented from regressing.

The multiple elitist strategies ME_1 and ME_2 are variants of the elitist selection strategy. With P equaling the size of the population, and given P parents and P children whose fitnesses are known, the number N_k between 1 and P of the best individuals from the union of the children and parents (size $2P$) are carried over to the next parent population. In both strategies the parents and children are ranked according to their fitnesses and the N_k best individuals become new parents. ME_1 and ME_2 differ in the way the $(P - N_k)$ remaining spots in the new parent population are filled. In ME_1 they are filled with the $(P - N_k)$ best children that are still available for selection, while in ME_2 they are filled with $(P - N_k)$ children selected randomly from the remaining ones. The choice of N_k is crucial since it affects the reliability of the algorithm and the richness of the population. Soremekun et al. [16] have proved that the choice $N_k \ll P$ ensures reliability of the multiple elitist selection schemes while maintaining enough richness. They used $P = 20$ and $N_k = 4$ in one of their studies and here we take $P = 16$ and $N_k = 3$ which gives the ratio N_k/P about the same as that in Soremekun et al. [16].

2.3.2. Formation of the children

Starting with a parent population the goal is to create a children population by combining genes of the parents giving preference to the best parents. The different steps are selection for mating, combination, and mutation.

The roulette-wheel selection is used to select two parents for mating. The probability is biased such that the best parents have more chance of being selected than parents with lower fitness. After ranking the parent population according to their fitness the ith best parent is given the fraction

$$p_i = \frac{2(P+1-i)}{P(P+1)} \tag{2}$$

of the roulette-wheel. Formally, the interval $[\varphi_{i-1}, \varphi_i[$ is attributed to the ith best parent where $\varphi_0 = 0$ and $\varphi_i = \varphi_{i-1} + p_i$. Then, a random number in $[0,1[$ is generated and the parent whose interval contains this number is selected. To form a pair of parents for mating the roulette-wheel selection is repeated until two distinct parents are selected.

The mating parents are then combined to form two children. We use here one-point crossover: a position is randomly chosen along the chromosome of one mating parent and the tails of the parent chromosomes (i.e., the genes located after the chosen position) are exchanged. Two children are created in this process, thus the size of the population remains constant. The purpose of the crossover is to exchange good building blocks between individuals to explore new designs.

A small variability is added by mutations in order to create new designs throughout the generations. Each gene of each child has a fixed small probability of undergoing mutation. If a gene is selected for mutation its value is randomly changed to a different one.

Specific operators tailored for stacking sequence optimization of laminates have been introduced, such as ply addition, deletion, swap and permutation (e.g., see Adams et al. [23]). They are, however, not included in the present study.

There is a chance that the new designs created after crossover and mutation do not satisfy the condition (1d). The children that violate this constraint go through the process described below before being included in the new parent population.

2.3.3. Constraints

The simple bound constraints listed in Eq. (1b) and (1c) are not violated by crossover or mutation. However, the constraint given by Eq. (1d) that PMMA and PC layers do not have common interfaces is more complex. Rather than using a penalty-method we adopt a repair technique to satisfy this constraint. After the children are born their genes are modified to respect Eq. (1d). Michalewicz [24] and Michalewicz and Schoenauer [25] used a reparation method to satisfy constraints, and Coello [26] and Watanabe [27] have reported that the reparation algorithm is a good choice when an infeasible solution can be easily transformed into a feasible solution. A limitation of this method, however, is that the repair algorithm is problem-specific. Here we use a reparation algorithm to remove constraint violations while preserving (as far as possible) the total number of PC and PMMA layers and their relative positions since they dominantly contribute to the energy dissipated during the impact. When needed, the following procedure is followed to repair the chromosomes. When two consecutive layers are made of the same material, one of these layers is deleted and the "empty space" created in the chromosome is used to shift the genes and insert an adhesive (randomly IM800A or DFA4700) layer at a PMMA/PC interface. If the constraint is still violated after this step then we look for and delete consecutive layers made of either the PMMA or the PC. If all constraints are still not satisfied then the algorithm replaces the material of one layer at each remaining PMMA/PC interface with an adhesive. Thus the constraints are always respected. The rationale for these modifications is that viscous deformations of the adhesive materials dissipate negligible amount of energy and their purpose is only to bond the PMMA and the PC layers. It was observed that in most cases the first two steps suffice to satisfy all constraints. Thus the reparation method described here has the advantage of rarely modifying the number of the PMMA and the PC layers or their respective positions within the plate.

2.3.4. Fitness evaluation

For the problem studied here, the fitness of an individual is the amount of energy dissipated during the impact event. This energy is numerically evaluated using the finite element (FE) software LS-DYNA. The computational cost is reduced by studying deformations of a quarter of the plate-impactor system with symmetry boundary conditions applied on appropriate surfaces and using a coarse FE mesh of 35,854 elements. The thickness of each layer is discretized using two 8-node brick elements with one integration point in each element. A minimum of two such FEs through the thickness are needed to consider the bending stiffness of a layer. Elements have nearly 1:1:1 aspect ratio in the vicinity of the center of impact. Results for the optimized configuration are checked by using a finer FE mesh as described in Section 3. Computing the fitness values of the 16 members of a generation requires about 1.5 h clock time with the MPP version of LS-DYNA on 48 Intel Xeon 2.5 GHz processors with a FDR-10 (40Gbps) Infiniband.

One of the outputs of LS-DYNA is the eroded energy of deleted elements that form cracks. For the intact elements the energy dissipated per unit volume due to plastic and viscous deformations is found, and the total dissipated energy is determined.

The GA software has been developed in FORTRAN. The population fitness (i.e., the energy dissipated) is found as described in the preceding paragraph. The GA forms the new population which is used in the FE simulations, and the cycle repeated till the optimum solution has been found as described in the flow chart of Fig. 2.

3. Results and discussion

3.1. Performance of the algorithm

Four optimizations for each selection scheme, ME_1 and ME_2, have been carried out. The maximum number of generations is set to 100 and the mutation probability to 0.0833 (one mutation per individual on average). In Fig. 3 we show the average of the best individuals of each optimization run and the overall best individual as a function of the generation for the two selection schemes.

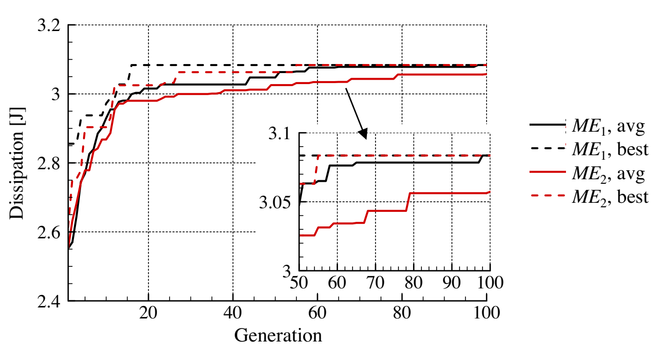

Fig. 3. Maximum and average fitness of the best individuals of the populations as a function of the generation number.

Design improvements obtained with the optimization algorithm are summarized in Table 2. The best initial fitness and the best final fitness as well as the corresponding relative improvement are given for each run.

About 20% improvement in the laminate performance could be obtained in all cases in less than 100 generations. The four runs using the ME_1 selection scheme yielded the same best design (see Table 3) and energy dissipation = 3.08 J. This design was found in two runs using ME_2 while the two remaining runs did not find it and yielded sub-optimal designs (see Table 3).

In order to analyze the energy dissipated in different layers of the best design, and to verify the accuracy of the energy dissipation, an impact simulation using the best design and a finer mesh was performed. The number of FEs in each spatial direction is multiplied by 1.5 to give a mesh with 116,644 elements versus 35,854 for the initial mesh. Note that in the initial mesh there are two elements through the thickness of each layer while the finer mesh has three elements. The total energy dissipated using the finer mesh was found to be 2.98 J which is 3.3% less than that found with the coarse mesh. This shows that the simulations using the coarse mesh provided reasonable values of the dissipated energy and hence the population fitness.

3.2. Analysis of the best design

For the best design configuration we have summarized in Table 4 the energy dissipated due to various mechanisms in each layer. It is clear that in the PMMA material, the energy is dissipated mainly through cracking (modeled with element deletion) while the energy dissipated due to its plastic deformations is small. The PC material can undergo large plastic deformations without failing and did not fail in the simulations. The eroded energy in the PC layers is null but that due to its plastic dissipation is large. The energy dissipated in the IM800A and DFA4700 adhesives is negligible. Therefore the main sources of energy dissipation are the cracking of the PMMA and plastic deformations of the PC, which agrees with the results presented in [22] for the impact of PMMA/IM800A/PC and PMMA/DFA4700/PC laminates (layer thicknesses 1.5875, 0.635 and 1.5875 mm, 28.5 g spherical impactor with 5 mm radius and 12 or 22 m/s impact velocity).

We now provide a few observations on the optimal design of the laminate. The optimal design has very few thin PC layers and thus will have large plastic deformations for maximizing the energy dissipated. This will degrade laminate response to subsequent impacts. However, that was not a design criterion for the problem studied. A possibility is to modify the design criterion in future for considering more than one impact.

The time history of the contact force between the plate and the impactor is shown in Fig. 4. There are two peaks separated by a local minimum ("valley") at time $t = 0.9$ ms. We note that the reaction force exhibits oscillations of increasing amplitude before reaching the first peak at 0.75 ms with magnitude 1.1 kN. The second peak of about 1.3 kN is reached at time $t = 1.15$ ms. Similar time histories of the contact force low velocity impacts of laminates have been reported in [28,29]. Parametric sensitivity studies

Table 2
Summary of design improvements.

	ME_1 selection scheme				ME_2 selection scheme			
	Run 1	Run 2	Run 3	Run 4	Run 1	Run 2	Run 3	Run 4
Best initial fitness [J]	2.54	2.40	2.42	2.86	2.60	2.56	2.43	2.61
Best final fitness [J]	3.08	3.08	3.08	3.08	3.03	3.08	3.03	3.08
Improvement	22%	29%	28%	8%	17%	20%	25%	18%

Table 3
Final designs found by the GA. The best design was found in all runs using ME_1 and two runs using ME_2. The remaining runs with ME_2 gave designs of rows 2 and 3 of the Table.

Fitness	Stacking sequence											
3.084 J	PC	IM	PC	IM	PMMA	IM	IM	PMMA	PMMA	PMMA	DFA	PC
3.032 J	PC	IM	PC	IM	PMMA	PMMA	IM	PMMA	PMMA	PMMA	DFA	PC
3.030 J	PC	IM	DFA	PC	IM	PC	IM	PMMA	PMMA	PMMA	PMMA	PMMA

Table 4
Energy dissipated in each layer for the best design computed with the fine FE mesh.

Layer #	Material	Eroded Energy (cracking) [J]	Plastic deformations [J]	Total [J]
1	PC	0.000	0.563	0.563
2	IM	0.000	0.000	0.000
3	PC	0.000	0.639	0.639
4	IM	0.000	0.000	0.000
5	PMMA	0.086	0.002	0.087
6	IM	0.000	0.000	0.000
7	IM	0.000	0.000	0.000
8	PMMA	0.105	0.001	0.106
9	PMMA	0.104	0.001	0.105
10	PMMA	0.113	0.002	0.115
11	DFA	0.000	0.000	0.000
12	PC	0.000	1.367	1.367
Total [J]		0.407	2.575	2.982

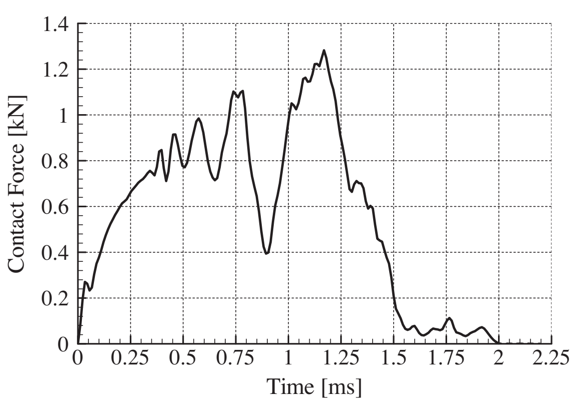

Fig. 4. Time history of the reaction force for the 20 m/s impact of the best design.

[31] have shown that the magnitude of the 1st peak and the subsequent valley but not of the 2nd peak in the reaction force time history can be accurately expressed as functions of material parameters of the constituents of the plate. However, the 2nd peak in the reaction force time history is correlated with the energy dissipated in the plate.

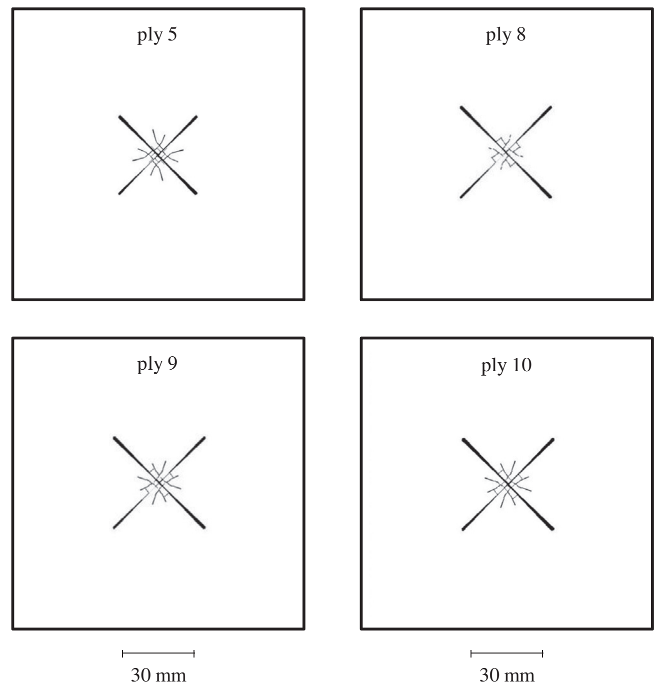

Fig. 6. Crack pattern in the PMMA material of the 5th, 8th, 9th and 10th layers.

Contours of the effective plastic strain in the PC layers near the center of impact are exhibited in Fig. 5 and crack patterns in the PMMA material of the 5th, 8th, 9th and 10th layers are shown in Fig. 6.

The largest effective plastic strains in the 1st, 3rd and 12th layers are 1.31, 1.40 and 1.38, respectively. The plastic deformations are highly localized in layers 1 and 3 and become negligible 5 mm away from the center of impact. In the rear layer, however, significant plastic deformations occur within 25 mm from the plate center. The crack patterns of plies 5 and 10 are comparable in terms of general appearance (long radial cracks and short secondary cracks that bifurcate) as well as length of the cracks. Penalizing the crack length in the objective function could give designs with smaller crack lengths which is an advantage since they degrade the transparency of the laminate.

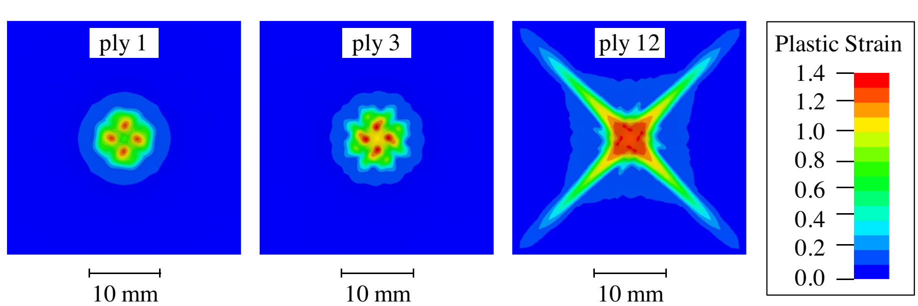

Fig. 5. Details of the effective plastic strains in the PC layers of the best design.

4. Conclusions

The mathematical and computational models of the low-velocity impact of poly-methyl-metha-acrylate (PMMA)/adhesive/polycarbonate (PC) laminate developed previously have been supplemented with a genetic algorithm (GA) to find the layup of layers of the materials involved that will maximize the energy dissipated during the deformations. It has been assumed that all layers have the same thickness, the total number of layers is fixed, the adjacent PMMA and the PC layers must have an adhesive layer between them, and the top and the bottom layers are not adhesive. It is found that 20% increase in the value of the objective function (energy dissipated) could be achieved in 100 generations. Values of the energy dissipated in each layer for the best design have shown that the PC layer has the most energy dissipated, and the viscous adhesive layers the least. Contrary to the laminate configuration often used in experiments, the layup with the PC rather than the PMMA layer at the top impacted surface enhances the energy dissipated. It is primarily due to the observation that the brittle failure of the PMMA layer consumes very little energy as compared to that need to plastically deform the PC layer. The significance of the work is in optimizing the design of a laminate whose constituents undergo large transient thermo-elasto-visco-plastic deformations.

Acknowledgments

This research was sponsored by the Army Research Laboratory and was accomplished under Cooperative Agreement Number W911NF-06-2-0014. The views and conclusions contained in this document are those of the authors and should not be interpreted as representing the official policies, either expressed or implied, of the Army Research Laboratory or the U.S. Government. The U.S. Government is authorized to reproduce and distribute reprints for Government purposes notwithstanding any copyright notation hereon.

References

[1] A. Florence, Interaction of projectiles and composite armour, part II. Standard Research Institute Menlo Park, California, in AMMRC-CR-69-15, 1969.
[2] Ben-Dor G, Dubinsky A, Elperin T, Frage N. Optimization of two component ceramic armor for a given impact velocity. Theor Appl Fract Mech 2000;33:185–90.
[3] Ben-Dor G, Dubinsky A, Elperin T. Optimization of two-component composite armor against ballistic impact. Compos Struct 2005;69:89–94.
[4] Hetherington JG. The optimization of two component composite armors. Int J Impact Eng 1992;12:409–14.
[5] Batra RC, Jin J. Natural frequencies of a functionally graded anisotropic rectangular plate. J Sound Vib 2005;282:509–16.
[6] Qian LF, Batra RC. Design of bidirectional functionally graded plate for optimal natural frequencies. J Sound Vib 2005;280:415–24.
[7] Goupee AJ, Vel SS. Two-dimensional optimization of material composition of functionally graded materials using meshless analyses and a genetic algorithm. Comput Method Appl M 2006;195:5926–48.
[8] Batra R. Optimal design of functionally graded incompressible linear elastic cylinders and spheres. AIAA J 2008;46:2050–7.
[9] Nagendra S, Haftka RT, Gurdal Z. Genetic algorithms for the design of composite panels. Eng Appl Fract Mech 1995;14:129–43.
[10] Nagendra S, Haftka RT, Gurdal Z. Stacking-sequence optimization of simply supported laminates with stability and strain constraints. AIAA J 1992;30:2132–7.
[11] Gantovnik VB, Anderson-Cook CM, Gurdal Z, Watson LT. A genetic algorithm with memory for mixed discrete–continuous design optimization. Comput Struct 2003;81:2003–9.
[12] Nagendra S, Jestin D, Gurdal Z, Haftka RT, Watson LT. Improved genetic algorithm for the design of stiffened composite panels. Comput Struct 1996;58:543–55.
[13] Kogiso N, Watson LT, Gürdal Z, Haftka RT, Nagendra S. Design of composite laminates by a genetic algorithm with memory. Mech Compos Mater Struct 1994;1:95–117.
[14] Gantovnik VB, Gurdal Z, Watson LT. A genetic algorithm with memory for optimal design of laminated sandwich composite panels. Compos Struct 2002;58:513–20.
[15] Malott B, Averill R, Goodman E, Ding Y, Punch W. Use of genetic algorithms for optimal design of laminated composite sandwich panels with bending-twisting coupling. In: Proceedings of 37th AIAA/ASME/AHS/ASC structures, structural dynamics, and materials conference, Salt Lake City, UT; 1996. pp. 1874–81.
[16] Soremekun GA, Gürdal Z, Haftka RT, Watson LT. Improving genetic algorithm efficiency and reliability in the design and optimization of composite structure, Department of computer science, Virginia Polytechnic Institute and State University; 1996.
[17] Punch WF, Averill RC, Goodman ED, Lin SC, Ding Y, Yip YC. Optimal-design of laminated composite structures using coarse-grain parallel genetic algorithms. Comput Syst Eng 1994;5:415–23.
[18] Punch WF, Averill RC, Goodman ED, Lin SC, Ding Y. Using genetic algorithms to design laminated composite structures. IEEE Expert 1995;10:42–9.
[19] Poirier JD, Vel SS, Caccese V. Multi-objective optimization of laser-welded steel sandwich panels for static loads using a genetic algorithm. Eng Struct 2013;49:508–24.
[20] Mulliken AD, Boyce MC. Mechanics of the rate-dependent elastic–plastic deformation of glassy polymers from low to high strain rates. Int J Solids Struct 2006;43:1331–56.
[21] Varghese AG, Batra RC. Constitutive equations for thermomechanical deformations of glassy polymers. Int J Solids Struct 2009;46:4079–94.
[22] Antoine GO, Batra RC. Low speed impact of laminated polymethylmethacrylate/adhesive/polycarbonate plates. Compos Struct 2014;116:193–210.
[23] Adams DB, Watson LT, Gurdal Z. Optimization and blending of composite laminates using genetic algorithms with migration. Mech Adv Mater Struct 2003;10:183–203.
[24] Michalewicz Z. A survey of constraint handling techniques in evolutionary computation methods. In: Proceedings of the 4th annual conference on evolutionary programming, Cambridge, MA: MIT Press; 1995. pp. 135–155.
[25] Michalewicz Z, Schoenauer M. Evolutionary algorithms for constrained parameter optimization problems. Evol Comput 1996;4:1–32.
[26] Coello CAC. Theoretical and numerical constraint-handling techniques used with evolutionary algorithms: a survey of the state of the art. Comput Method Appl M 2002;191:1245–87.
[27] Watanabe K, Hashem MMA. Evolutionary computations: new algorithms and their applications to evolutionary robots. Berlin; New York: Springer; 2004.
[28] Stenzler JS, Goulbourne N. Impact mechanics of transparent multi-layered polymer composites. In: Society for experimental mechanics-sem annual conference and exposition on experimental and applied mechanics; 2009. p. V3.
[29] Wu HYT, Chang FK. Transient dynamic analysis of laminated composite plates subjected to transverse impact. Comput Struct 1989;31:453–66.
[30] Antoine GO, Batra RC. Constitutive relations and parameter estimation for finite deformations of viscoelastic adhesives. ASME - J Appl Mech 2015;82. Art. No. 021001.
[31] Antoine GO, Batra RC. Sensitivity analysis of low-velocity impact response of laminated plates. Int J of Impact Eng 2015;78:64–80.